

## PHOTOCATALYTIC PROPERTIES OF CoO/g-C<sub>3</sub>N<sub>4</sub> NANOCOMPOSITES MODIFIED BY CARBON QUANTUM DOT

X. H. ZHANG, Y. L. ZHUANG, W. SUN, X. J. LI, L. W. SHAN, L. M. DONG\*  
*College of Materials Science and Engineering, Harbin University of Science and  
Technology, Harbin 150040, China.*

A CQDs/CoO/g-C<sub>3</sub>N<sub>4</sub> nanocomposite used for photocatalytic degradation was designed and fabricated in this paper. The effects of carbon quantum dots (CQDs) content and synthesis temperature on photocatalytic properties of nanocomposites were studied. The results show that the solar energy utilization efficiency of CQDs/CoO/g-C<sub>3</sub>N<sub>4</sub> nanocomposite is twice that of pure g-C<sub>3</sub>N<sub>4</sub> when the content of CQDs is 4.5 wt%. The improvement of photocatalytic performance of nanocomposite is mainly attributed to the synergistic effect of the junction/interface between g-C<sub>3</sub>N<sub>4</sub>, CoO and CQDs.

(Received August 5, 2020; Accepted October 11, 2020)

*Keywords:* Photocatalyst, CQDs/CoO/g-C<sub>3</sub>N<sub>4</sub> nanocomposite, Methylene blue

### 1. Introduction

With the progress and development of today's society, people's living standards have also improved, which has resulted in increased consumption of cosmetics, clothes, etc. However, manufacturers that produce these items will use a lot of toxic or durable materials, which will cause serious pollution of water resources [1-3]. In order to protect our water resources and reduce pollution, in the past few decades, various practical sewage treatment technologies have been implemented [4-6]. So far, photocatalysis technology has been considered as one of the most effective wastewater treatment programs because it has great potential and high efficiency, and can use sunlight to remove organic pollutants with the help of solid photocatalysts [7,8]. Among them, as a metal-free organic polymer semiconductor, graphitized carbon nitride (g-C<sub>3</sub>N<sub>4</sub>) has been widely used in the research of photocatalytic degradation of pollutants and hydrogen evolution due to its advantages of non-toxicity, stability, reliability and low cost [9,10]. The band gap of the photocatalytic material g-C<sub>3</sub>N<sub>4</sub> (2.7eV) is relatively narrow, with suitable conduction band and valence band to capture the UV-Vis light in sunlight to degrade pollutants [11,12]. However, the rapid recombination of photo-generated carriers, poor UV-visible light utilization rate and low specific surface area severely restrict the photocatalytic degradation efficiency of materials [13]. To overcome these difficulties, researchers have developed various strategies to improve the photocatalytic activity of g-C<sub>3</sub>N<sub>4</sub>, such as the preparation of nanostructures [14], coupling [15],

---

\* Corresponding author: donglm@hrbust.edu.cn

doping [16], and compounding with other semiconductor materials [17]. It is worth noting that the combination of g-C<sub>3</sub>N<sub>4</sub> with other semiconductor materials can significantly improve the photocatalytic activity [17,18].

In recent years, because Bao et al. found that CoO has a strong photocatalytic capability, CoO photocatalysts have attracted more and more attention from the scientific community. The reported cobalt oxide material can completely decompose water through the photocatalytic process, with unprecedented solar energy conversion efficiency (STH=5%) [19]. However, there are few reports on the study of CoO as an organic photocatalyst to degrade pollutants. This may be mainly due to the low valence state of cobalt in CoO materials, the material is more difficult to synthesize, and the synthesized CoO nanoparticles are seriously aggregated. The stability of the catalyst is also relatively poor, and it is easy to be seriously deactivated, which hinders the further development of the material. Fortunately, g-C<sub>3</sub>N<sub>4</sub> with a large specific surface area and 2D structure can provide a large scaffold for fixing CoO matrix, which can not only effectively prevent the aggregation of nanoparticles, but also enhance the photocatalytic activity and stability of the material [20]. Although there are scientists working on CoO/g-C<sub>3</sub>N<sub>4</sub> materials to degrade pollutants [21], the results of photocatalysis are still not high and need further optimization.

Carbon quantum dots (CQDs) are a new type of spherical carbon, containing amorphous nanocrystalline nuclei, with typical graphite carbon (sp<sup>2</sup> carbon), a new type of carbon nanoparticles formed by fusion of diamond-like sp<sup>3</sup> hybrid carbon inserts material. Due to its low toxicity, biocompatibility, low cost, chemical inertness, and fluorescence characteristics, it has gradually replaced traditional semiconductor quantum dots [22]. Carbon quantum dots are widely used in photocatalysis, electrocatalysis, and fluorescence imaging due to their excellent characteristics (high water solubility, strong size effect, up-conversion photoluminescence behavior) [23]. In terms of photocatalysis, CQDs are a good electron buffer, which allows semiconductor materials to continuously receive or provide electrons [24,25]. In addition, due to the  $\pi$  bond conjugated structure and rich oxygen-containing groups on the surface, This makes quantum dots easier to combine with semiconductors [26,27]. In addition, CQDs can convert near-infrared to visible light, which in turn is absorbed by CoO/g-C<sub>3</sub>N<sub>4</sub>, thereby enhancing the subsequent photocatalytic effect.

In this study, a new CQDs/CoO/g-C<sub>3</sub>N<sub>4</sub> composite photocatalytic material was prepared by solvent thermal reaction. The effects of the addition amount of CQDs and the synthesis process on the photocatalytic properties of composites were studied. The degradation of MB in visible light ( $\lambda < 420\text{nm}$ ) was studied to characterize the photocatalytic performance of composites.

## 2. Experiment

The main raw materials for the preparation of composite materials are melamine (AR) (Tianjin Hengxing Chemical Reagent co., Ltd., China), C<sub>6</sub>H<sub>8</sub>O<sub>7</sub>·H<sub>2</sub>O (AR), Co(NO<sub>3</sub>)<sub>2</sub>·6H<sub>2</sub>O (AR), EDTA (AR), tert-butanol (AR) (Tianjin Fuchen Chemical Reagent co., Ltd., China), MB (Tianjin Jinfeng Chemical co., Ltd., China), L-cys (98.5%) (Tianjin Guangfu Fine Chemical Research Institute, China) and P-quinone (99%) (McLean Reagent Company, China).

First, weigh 1.05 g of C<sub>6</sub>H<sub>8</sub>O<sub>7</sub>·H<sub>2</sub>O and 0.61 g of L-cys and grind them thoroughly. Keep the ground mixed powder in an incubator at 200 °C for 210 min and then cooled to room

temperature. Add 100 ml deionized water to the mixed powder and stir for 30 min. Then a 0.22  $\mu\text{m}$  filter membrane was used for extraction. The filtrate was placed in an incubator at 70  $^{\circ}\text{C}$  to dry for 12 h to obtain solid CQDs.

Second, Weigh 10 g  $\text{C}_3\text{N}_3\cdot(\text{NH}_2)_3$  into the crucible, then put the crucible into the muffle furnace at 500  $^{\circ}\text{C}$  (2.5  $^{\circ}\text{C}\cdot\text{min}^{-1}$ ) for 6 h. Cooling to room temperature will yield a g-C<sub>3</sub>N<sub>4</sub> powder.

The first step is to synthesize CoO/g-C<sub>3</sub>N<sub>4</sub> composite. According to literature, the photocatalytic performance of CoO/g-C<sub>3</sub>N<sub>4</sub> composite material is better when the content of CoO is 0.5 wt% [28]. Therefore, CoO(0.5 wt%)/g-C<sub>3</sub>N<sub>4</sub> is selected as the matrix of ternary composite in this experiment. The synthesis process was as follows: firstly, 0.024 g cobalt nitrate hexahydrate was fully dissolved in 15 ml deionized water to form cobalt nitrate solution. Secondly, 1.2 g g-C<sub>3</sub>N<sub>4</sub> was dissolved in cobalt nitrate solution, ultrasonic for 10 min and magnetic stirring for 10 min. The aqueous solution was then vaporized and cured in a constant temperature water bath. The solidified powder was ground and then put into muffle furnace for sintering. The sintering process was kept at 300  $^{\circ}\text{C}$  for 2 h, and then cooled to room temperature with the furnace. After full grinding, CoO(0.5 wt%)/g-C<sub>3</sub>N<sub>4</sub> composite was obtained.

The second step is to Synthesis of CQDs/CoO/g-C<sub>3</sub>N<sub>4</sub> composite materials. CQDs with different contents (1.5 wt%, 2.5 wt%, 3.5 wt%, 4.5 wt% and 5.5 wt%) were mixed with CoO(0.5 wt%)/g-C<sub>3</sub>N<sub>4</sub>, and the mixed powder was added to ethanol (40 ml) and deionized water (40 ml) to form a mixed solution. After 30 min of ultrasound and 20 min of magnetic stirring, the mixed solution was transferred to the polytetrafluorin reactor. The mixed solution was kept under temperatures 200  $^{\circ}\text{C}$  for 4 h and cooled to room temperature. The reactants were centrifuged for washing and dried at 60  $^{\circ}\text{C}$  for 12 h to obtain CQDs/CoO/g-C<sub>3</sub>N<sub>4</sub> composite material samples.

The experiment was performed using X'Pert PRO type X-ray diffractometer from Panalytical Analytical Instrument Company of the Netherlands. The sample powder X-ray diffraction (XRD) was recorded under the conditions of target material: Cu K $\alpha$  ( $\lambda = 1.5406\text{\AA}$ ), output power: 300KW) mode. A field emission scanning electron microscope (FE-SEM, Sirion200, Philip) and a transmission electron microscope (TEM, JEM2100, Japan) were used to observe and analyze the microstructure of the material. A 150W xenon lamp with a wavelength of 335 nm was used as an excitation source, and the photoluminescence spectrum (PL, RF-5301PC, Shimadzu, Japan) was measured at an excitation wavelength of 375 nm at room temperature

The catalytic experiment used a 300 W xenon lamp for simulated sunlight. First, 0.1 g of the experimental sample was weighed and dispersed in 100 mL of a 10 mg/L methylene blue solution, and then stirred for 60 min in the dark to ensure the establishment of an adsorption-desorption balance. Xenon lamps were then turned on for photocatalytic experiments. At a specific time interval, remove a certain amount of solution into the cuvette via a pipette. Then, the characteristic absorption value of methylene blue at 664 nm was measured on a UV-vis spectrophotometer. Finally, the photocatalytic degradation rate (DR%) was calculated by the following formula:

$$DR = [1 - (A/A_0)] \times 100\% \quad (1)$$

where  $A_0$  is the UV-vis absorption of the original solution of pollutants that reached absorption equilibrium, and  $A$  is the UV-vis absorption of degraded solution at the certain time. Cyclic test was used to test the service life of the material. Photocatalytic capture agents such as

benzoquinone, tert-butanol alcohol and EDTA-2Na were used to capture active substances, and the effects of the active substances on solution degradation were studied [29].

### 3. Results and discussion

Fig. 1 shows the XRD diffraction patterns of g-C<sub>3</sub>N<sub>4</sub>, CoO/g-C<sub>3</sub>N<sub>4</sub> and CQDs/CoO/g-C<sub>3</sub>N<sub>4</sub> ternary samples with different CQDs contents. It can be seen that pure g-C<sub>3</sub>N<sub>4</sub> has two typical diffraction peaks at  $2\theta=27.73^\circ$  (002) and  $12.8^\circ$  (100), which are ascribed to the layer stacking of conjugated aromatic rings, and the in-plane trigonal nitrogen linkage of tri-s-triazine motifs on g-C<sub>3</sub>N<sub>4</sub> respectively[28]. For 0.5% by weight CoO/g-C<sub>3</sub>N<sub>4</sub> composites, the characteristic peaks of g-C<sub>3</sub>N<sub>4</sub> can be clearly observed, which indicates that CoO/g-C<sub>3</sub>N<sub>4</sub> composites have good g-C<sub>3</sub>N<sub>4</sub> basic structure. The characteristic peak of CoO are not very obvious, which may be caused by the low crystallinity of CoO. In the experiment, a composite material with a content of 10 wt% CoO/g-C<sub>3</sub>N<sub>4</sub> was made separately. According to the PDF card (JCPDS 75-0393), it can be clearly seen that the  $2\theta$  of CoO is  $36.5^\circ$ (111) and  $42.4^\circ$ (200) With two characteristic peaks, CoO/g-C<sub>3</sub>N<sub>4</sub> composites were successfully prepared [30].As the amount of CQDs increased, the phase structure of g-C<sub>3</sub>N<sub>4</sub> is still well retained, but the characteristic peak of graphitic carbon has not been observed in the spectrum, perhaps this is because of the low dosage of CQDs or amorphous carbon in a significant portion [31].

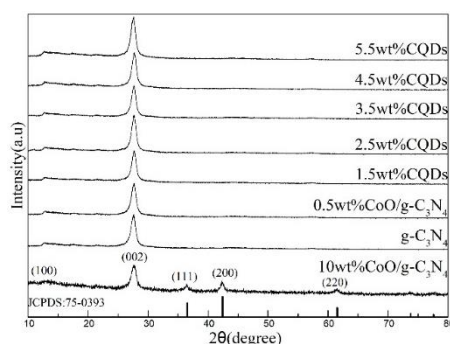
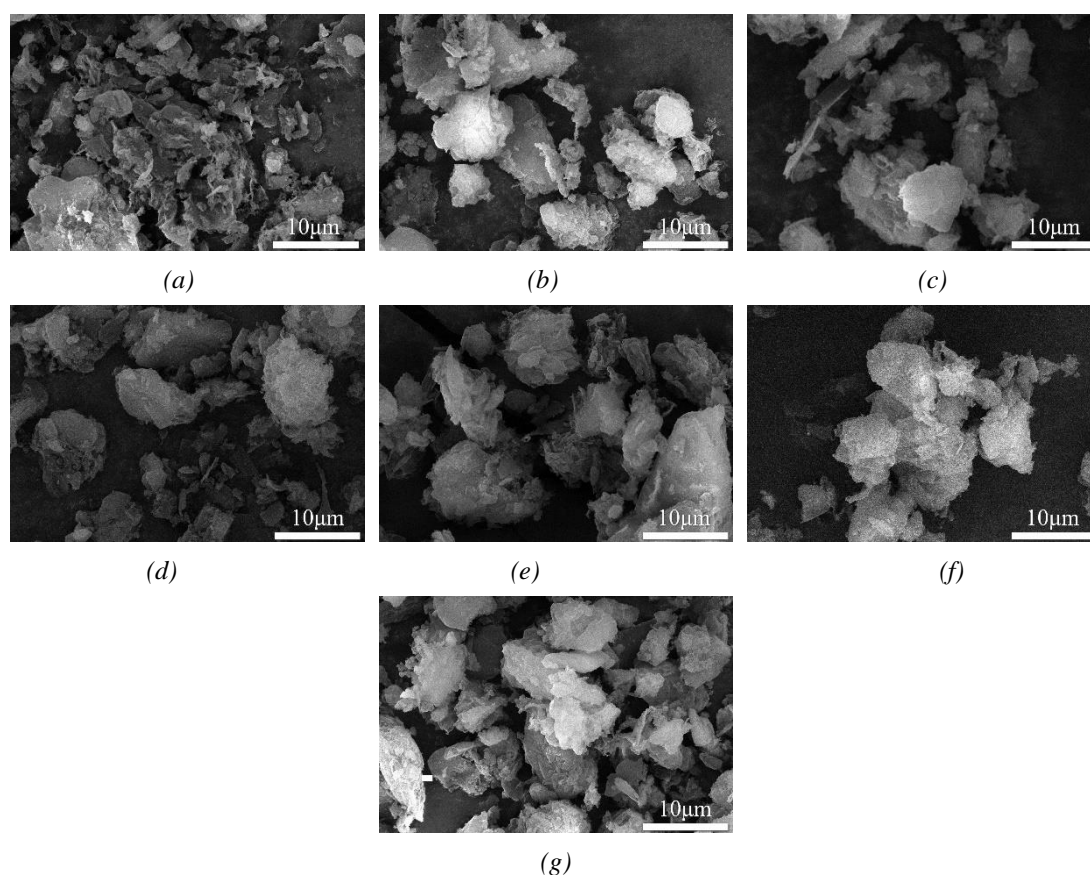


Fig. 1. XRD patterns of the pure g-C<sub>3</sub>N<sub>4</sub>, CoO/g-C<sub>3</sub>N<sub>4</sub> and CQDs/CoO/g-C<sub>3</sub>N<sub>4</sub> composites with different doping amounts of CQDs.

Fig. 2 shows the morphology of pure g-C<sub>3</sub>N<sub>4</sub>, CoO/g-C<sub>3</sub>N<sub>4</sub> and CQDs/CoO/g-C<sub>3</sub>N<sub>4</sub> composites with different CQDs contents. It can be seen from Fig. 2(a), the g-C<sub>3</sub>N<sub>4</sub> is stacked in a two-dimensional layered structure, some of them are like flocculent particles gathered on two-dimensional flakes, and some nano-scale pore structures can also be observed between two-dimensional flakes. CoO/g-C<sub>3</sub>N<sub>4</sub> is a two-dimensional sheet structure (as shown in Fig. 2(b)). From Fig. 2(c-g) can be seen that the morphologies of CQDs/CoO/g-C<sub>3</sub>N<sub>4</sub> with different CQDs contents change very little, and there is almost no obvious change compared with pure g-C<sub>3</sub>N<sub>4</sub>. In order to further analyze the morphology and interface formation of CQDs(4.5wt%)/CoO/g-C<sub>3</sub>N<sub>4</sub> composite materials, transmission electron microscope was used [32]. The result is shown in Fig. 3. It can be seen that g-C<sub>3</sub>N<sub>4</sub> has a nanoscale structure, CQDs and CoO nanoparticles are attached to

the surface of g-C<sub>3</sub>N<sub>4</sub>. The average sizes of CQDs and CoO nanoparticles are about 14 nm and 15 nm, respectively.

Fig. 4 shows the photocatalytic degradation efficiency of pure g-C<sub>3</sub>N<sub>4</sub>, CoO/g-C<sub>3</sub>N<sub>4</sub> and CQDs/CoO/g-C<sub>3</sub>N<sub>4</sub> doped with different amounts of CQDs under visible light. It can be seen from the figure that the adsorption and degradation efficiency of pure g-C<sub>3</sub>N<sub>4</sub> is relatively low, about 16% and 22%, and the final degradation rate is 38%. According to previous studies, 0.5 wt% CoO was incorporated into g-C<sub>3</sub>N<sub>4</sub>[28], the adsorption efficiency and photocatalytic efficiency of the material were significantly improved. Compared with the pure g-C<sub>3</sub>N<sub>4</sub>, the adsorption efficiency increased by 2 times, and the photocatalytic efficiency increased by 1.3 times. Then, based on CoO/g-C<sub>3</sub>N<sub>4</sub> with a CoO doping amount of 0.5 wt%, CQDs with different contents are doped. With the increasing content of CQDs, the adsorption effect and photocatalytic effect of the composite material will increase to a certain extent. When the doping amount is 4.5 wt%, the photocatalytic effect reaches 82% optimally, but when the content of CQDs increases to 5.5 wt%, the photocatalytic effect of the material drops to 65%. The results show that when doped with CQDs, the photocatalytic performance of the material increases relatively. When the doping amount of CQDs is 4.5 wt%, the photocatalytic performance of the material is the best.



*Fig. 2. Morphologies of of g-C<sub>3</sub>N<sub>4</sub>, CoO/g-C<sub>3</sub>N<sub>4</sub> and CQDs/CoO/g-C<sub>3</sub>N<sub>4</sub> CQDs with different CQDs contents: (a) g-C<sub>3</sub>N<sub>4</sub>, (b) CoO/g-C<sub>3</sub>N<sub>4</sub>, (c)-(g) The doped CQDs of CoO/g-C<sub>3</sub>N<sub>4</sub> CQDs are 1.5wt%, 2.5wt%, 3.5wt%, 4.5wt% and 5.5wt%, respectively.*

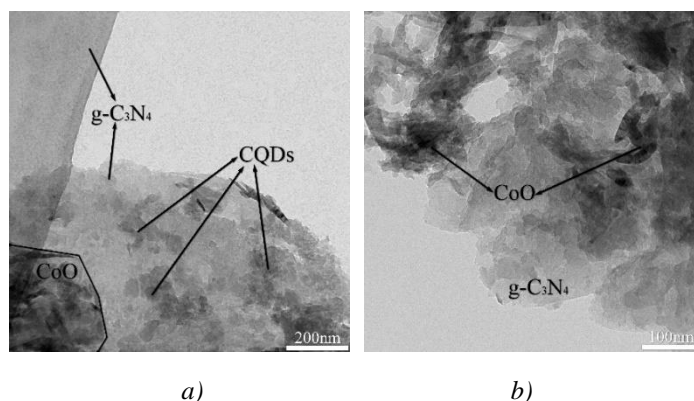


Fig. 3. TEM images of CQDs (4.5wt%)/CoO/g-C<sub>3</sub>N<sub>4</sub> composites ( $T=200\text{ }^{\circ}\text{C}$ ), (a) and (b) are respectively CQDs and CoO in the composites.

Fig. 5 shows the photoluminescence (PL) spectras of pure g-C<sub>3</sub>N<sub>4</sub> and CQDs/CoO/g-C<sub>3</sub>N<sub>4</sub> composites with different CQDs content. The excitation wavelength is 375 nm. It is well known that there is a strong correlation between fluorescence intensity and photocatalytic performance, and the fluorescence signal reveals the capture and recombination process of photogenic carrier in semiconductor photocatalyst [30]. The lower the PL excitation intensity is, the lower the recombination probability of photogenic carriers will be, and then more photogenic carriers will participate in the photocatalytic reaction, making them have higher photocatalytic activity. It can be seen from the Fig. 5 that all samples have obvious emission peaks at the excitation wavelength of 465 nm. Among them, the pure g-C<sub>3</sub>N<sub>4</sub> has the strongest emission intensity. The emission intensity of CQDs/CoO/g-C<sub>3</sub>N<sub>4</sub> with different CQDs contents samples are lower than that of pure g-C<sub>3</sub>N<sub>4</sub>. This indicates that CQDs/CoO/g-C<sub>3</sub>N<sub>4</sub> with different CQDs contents can effectively inhibit the recombination of electron-hole pairs. And when the CQDs content is 4.5 wt%, the photocatalytic activity of the CQDs/CoO/g-C<sub>3</sub>N<sub>4</sub> composite is the highest.

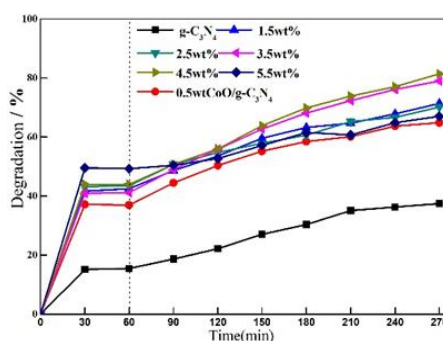


Fig. 4. Degradation curves of g-C<sub>3</sub>N<sub>4</sub>, CoO/g-C<sub>3</sub>N<sub>4</sub>, and CQDs/CoO/g-C<sub>3</sub>N<sub>4</sub> with different CQDs contents.

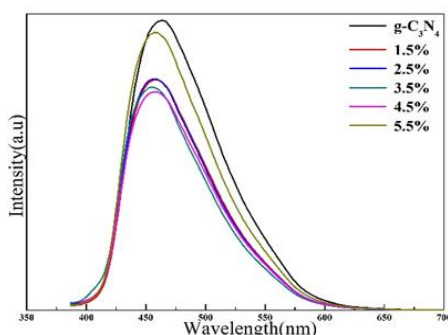


Fig. 5. Photoluminescence spectras of  $g\text{-C}_3\text{N}_4$  and  $\text{CQDs}/\text{CoO}/g\text{-C}_3\text{N}_4$  with different CQDs contents.

Then the repeated photocatalytic experiments on the prepared CQDs (4.5wt%)/CoO/ $g\text{-C}_3\text{N}_4$  were carried out. The cycle life and service stability of photocatalyst can be well tested by repeated experiments. In this paper, the MB solution of 10 mg/L was degraded repeatedly for 5 times by CQDs(4.5 wt%)/CoO/ $g\text{-C}_3\text{N}_4$  composites. The adsorption rate after 1 hour of the first dark treatment and the final degradation rate after 3.5 h were recorded, and the change of MB decolorization rate was observed. The result is shown in Fig. 6. It can be seen that the adsorption rate in the first three repeated experiments changed little, while it decreased rapidly in the fourth and fifth repeated experiments. Compared with the results of the first experiment, the adsorption rate of the fifth experiment decreased by 15.75%. At the same time, it can be seen that the second degradation of MB has the most obvious effect, which is 17.77% lower than the first degradation rate, and the fifth degradation rate is about 32.59% lower than the first. From the results of the cyclic experiment, the adsorption and degradation of MB decreased with the number of repetitions. However, the degradation rate of the last few times was maintained at about 20%, which indicated that the photocatalytic activity of the composites was still good. The reason for the decline in the final degradation rate may be that the quality of samples will be lost after washing after each degradation experiment. Moreover, after repeated washing, the sample surface may be left with unwashed MB, and the sample may be partially deactivated due to repeated use, all of which will reduce the photocatalytic activity of the sample. According to the literature, an appropriate amount of catalyst can be added in practical application to balance this loss [33,34].

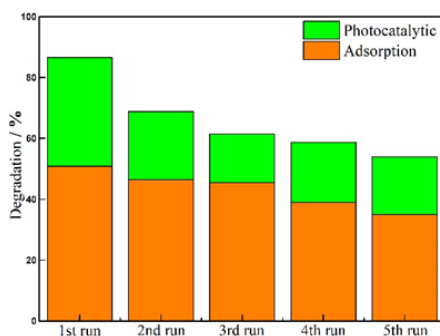


Fig. 6. Degradation rate of MB by  $\text{CQDs}(4.5\text{wt}\%)/\text{CoO}/g\text{-C}_3\text{N}_4$  in cyclic experiments.

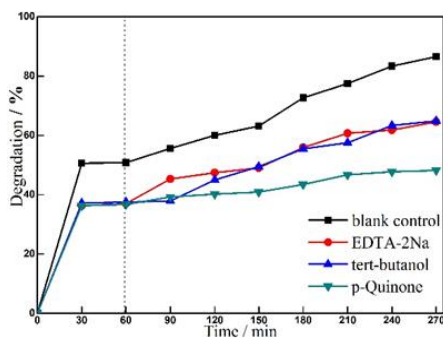
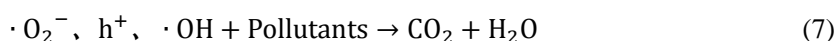
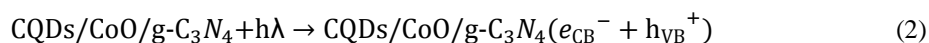


Fig. 7. Degradation rate of MB by CQDs(4.5wt%)/CoO/g-C<sub>3</sub>N<sub>4</sub> under different capture agents.

Fig. 7 shows the degradation rate of MB by CQDs (4.5 wt%)/CoO/g-C<sub>3</sub>N<sub>4</sub> under different capture agents. It can be seen that the degradation rate of MB solution without adding capture agent is about 86%, the degradation rates of EDTA-2Na and tert-butanol to MB solution is similar (about 65%), and the degradation rate of p-benzoquinone to MB solution is only 48.16%. According to the photocatalytic mechanism, the following reactions occur when light is irradiated on the surface of CQDs/CoO/g-C<sub>3</sub>N<sub>4</sub> composites:



By capturing hydroxyl radicals, reactive oxygen species and holes in the reaction process, the trapping agent reduces the corresponding active substances involved in the degradation of methylene blue solution, thus inhibiting the photocatalytic activity of the material. Thus, it can be explained that in the process of degradation of MB by CQDs (4.5 wt%)/CoO/g-C<sub>3</sub>N<sub>4</sub> composites, the oxidation of  $\cdot\text{O}_2^-$  free radical plays the most important role, and the oxidation of  $\cdot\text{OH}$  radical and holes is relatively weak.

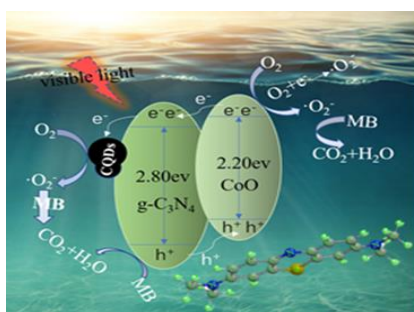


Fig. 8. Visible light photocatalytic mechanism of composite materials.

From the above analysis and discussion, a possible photocatalytic mechanism of CQDs/CoO/g-C<sub>3</sub>N<sub>4</sub> ternary composite photocatalytic material is proposed and shown in the figure. Since the CB edge potential of g-C<sub>3</sub>N<sub>4</sub> is more negative than that of CoO, the photo-generated electrons generated by CB of g-C<sub>3</sub>N<sub>4</sub> can be directly transferred to CoO under the irradiation of visible light. On the contrary, the VB of CoO will be transferred to g-C<sub>3</sub>N<sub>4</sub> by photo-generated holes generated by visible light irradiation. The electrons and holes transferred to CB and VB will undergo oxidation-reduction reactions to degrade MB. In addition, CQDs deposited on CoO/g-C<sub>3</sub>N<sub>4</sub> composite materials can play an active role in photocatalysis. On the one hand, CQDs can transfer electrons in photocatalysis, making electrons easier to transfer to the surface of CoO/g-C<sub>3</sub>N<sub>4</sub> materials, promoting the use of electrons and enhancing the separation of electron holes. On the other hand, the addition of CQDs can widen the range of the visible light absorption spectrum of the material, thereby exciting the material to generate more electron-hole pairs. Therefore, it can be concluded that the performance enhancement of the prepared photocatalytic materials is mainly due to the particularity of CQDs materials, so that the composite photocatalytic materials have great advantages in improving visible light absorption and charge separation rate.

#### 4. Conclusion

The CQDs/CoO/g-C<sub>3</sub>N<sub>4</sub> composite photocatalyst was synthesized by solvent heating method. The effect of CQDs content on the photocatalytic performance of composite materials was studied. The results show that when the CQDs content is 4.5 wt%, the synthesized composite material has the best photocatalytic effect, and the corresponding degradation rate is about 82%. Moreover, the phase and morphology of the composite material will not change significantly with the change of CQDs content. Cyclic testing shows that CQDs (4.5 wt%)/CoO/g-C<sub>3</sub>N<sub>4</sub> composite materials have good photocatalytic stability. The photocatalytic performance of the composite material is affected by the type of collector. During the degradation of MB by CQDs (4.5 wt%)/CoO/g-C<sub>3</sub>N<sub>4</sub> composites, the oxidation of ·O<sub>2</sub><sup>-</sup> radicals is the most important, while the oxidation of ·OH radicals and holes is relatively weak.

#### Acknowledgements

This project was supported by University Nursing Program for Young Scholars with Creative Talents in Heilongjiang Province(No.2018204), China Postdoctoral Science Foundation(No.2019M651940).

#### References

- [1] A. Y. Meng, L. Y. Zhang, B. Cheng, J. G. Yu, *Adv. Mater.* **31**, 31 (2019).
- [2] W. L. Yu, J. F. Zhang, T. Y. Peng, *Appl. Catal. B: Environ.* **181**, 220 (2016).
- [3] G. G. Tang, F. X. Zhang, P. W. Huo, S. Zulfiqarc, J. Xu, Y. S. Yan, H. Tang, *Ceram. Int.* **45**, 19197 (2019).

- [4] X. Zhou, Y. X. Li, Y. Zhao, *Rsc Advances* **4**, 15620 (2014).
- [5] V. K. Gupta, I. Ali, T. A. Saleh, A. Nayak, S. Agarwal, *Rsc Advances* **2**, 6380 (2012).
- [6] J. H. Sun, B. Zhang, R. X. Sun, Y. F. Li, J. F. Wu, *International Journal of Environment and Pollution* **38**, 81 (2009).
- [7] M. Tanveer, G. Tezcanli-Guyer, *Renewable & Sustainable Energy Reviews* **24**, 534 (2013).
- [8] L. Y. Yang, S. Y. Dong, J. H. Sun, J. L. Feng, Q. H. Wu, S. P. Sun, *Journal of Hazardous Materials* **179**, 438 (2010).
- [9] P. Chen, F. L. Wang, Q. X. Zhang, Y. H. Su, L. Z. Shen, K. Yao, Z. F. Chen, Y. Liu, Z. W. Cai, W. Y. Lv, G. G. Liu, *Chemosphere* **172**, 193 (2017).
- [10] Q. Liu, T. X. Chen, Y. R. Guo, Z. G. Zhang, X. M. Fang, *Applied Catalysis B-Environmental*, **193**, 248 (2016).
- [11] F. L. Wang, P. Chen, Y. P. Feng, Z. J. Xie, Y. Liu, Y. H. Su, Q. X. Zhang, Y. F. Wang, K. Yao, W. Y. Lv, G. G. Liu, *Applied Catalysis B-Environmental* **207**, 103 (2017).
- [12] Y. H. Su, P. Chen, F. L. Wang, Q. X. Zhang, T. S. Chen, Y. F. Wang, K. Yao, W. Y. Lv, G. G. Liu, *Rsc Advances* **7**, 34096 (2017).
- [13] C. Y. Liu, Y. H. Zhang, F. Dong, A. H. Reshak, L. Q. Ye, N. Pinna, C. Zeng, T. R. Zhang, H. W. Huang, *Applied Catalysis B-Environmental* **203**, 465 (2017).
- [14] C. Chang, Y. Fu, M. Hu, C. Y. Wang, G. Q. Shan, L. Y. Zhu, *Applied Catalysis B-Environmental* **142**, 553 (2013).
- [15] Y. B. Wang, X. Zhao, D. Cao, Y. Wang, Y. F. Zhu, *Applied Catalysis B-Environmental* **211**, 79 (2017).
- [16] L. Dong, D. Liu, H. Fu, X. Li, L. Shan, *Journal of Inorganic and Organometallic Polymers and Materials* **29**, 1297 (2019).
- [17] Y. Guo, J. Li, Z. Gao, X. Zhu, Y. Liu, Z. Wei, W. Zhao, C. Sun, *Applied Catalysis B-Environmental* **192**, 57 (2016).
- [18] Z. Y. Mao, J. J. Chen, Y. F. Yang, D. J. Wang, L. J. Bie, B. D. Fahlman, *Acs Applied Materials & Interfaces* **9**, 12427 (2017).
- [19] L. B. Liao, Q. H. Zhang, Z. H. Su, Z. Z. Zhao, Y. N. Wang, Y. Li, X. X. Lu, D. G. Wei, G. Y. Feng, Q. K. Yu, X. J. Cai, J. M. Zhao, Z. F. Ren, H. Fang, F. Robles-Hernandez, S. Baldelli, J. M. Bao, *Nature Nanotechnology* **9**, 69 (2014).
- [20] F. Guo, W. L. Shi, H. B. Wang, M. M. Han, H. Li, H. Huang, Y. Liu, Z. H. Kang, *Catalysis Science & Technology* **7**, 3325 (2017).
- [21] F. Guo, W. Shi, C. Zhu, H. Li, Z. Kang, *Applied Catalysis B-Environmental* **226**, 412 (2018).
- [22] S. Y. Lim, W. Shen, Z. Gao, *Chemical Society Reviews* **44**, 362 (2015).
- [23] H. J. Yu, R. Shi, Y. F. Zhao, G. I. N. Waterhouse, L. Z. Wu, C. H. Tung, T. R. Zhang, *Advanced Materials* **28**, 9454 (2016).
- [24] Y. J. Ma, X. L. Li, Z. Yang, S. S. Xu, W. Zhang, Y. J. Su, N. T. Hu, W. J. Lu, J. Feng, Y. F. Zhang, *Langmuir* **32**, 9418 (2016).
- [25] J. J. Wang, L. Tang, G. M. Zeng, Y. C. Deng, H. R. Dong, Y. N. Liu, L. L. Wang, B. Peng, C. Zhang, F. Chen, *Applied Catalysis B-Environmental* **222**, 115 (2018).
- [26] L. Shan, C. Lu, L. Dong, J. Suriyaprakash, *Journal of Alloys and Compounds* **804**, 385 (2019).
- [27] F. L. Wang, P. Chen, Y. P. Feng, Z. J. Xie, Y. Liu, Y. H. Su, Q. X. Zhang, Y. F. Wang, K. Yao, W. Y. Lv, G. G. Liu, *Applied Catalysis B-Environmental* **207**, 103 (2017).

- [28] Y. Hou, Y. Zhu, Y. Xu, X. Wang, *Applied Catalysis B-Environmental* **156**, 122 (2014).
- [29] J. Li, Q. Zhou, F. Yang, L. Wu, W. Li, R. Ren, Y. Lv, *New Journal of Chemistry* **43**, 14829 (2019).
- [30] Z. Y. Mao, J. J. Chen, Y. F. Yang, D. J. Wang, L. J. Bie, B. D. Fahlman, *Acs Applied Materials & Interfaces* **9**, 12427 (2017).
- [31] J. Y. Qin, H. P. Zeng, *Applied Catalysis B-Environmental* **209**, 161 (2017).
- [32] X. C. Liu, Q. Zhang, L. W. Liang, L. T. Chen, Y. Y. Wang, X. Q. Tan, L. Wen, H. Y. Huang, *Royal Society Open Science* **6**, (2019).
- [33] J. Li, F. Yang, Q. Zhou, R. Ren, L. Wu, Y. Lv, *Journal of Colloid and Interface Science* **546**, 139 (2019).
- [34] A. Phuruangrat, K. Karthik, B. Kuntalue, P. Dumrongrojthanath, S. Thongtem, T. Thongtem, *Chalcogenide Letters*, **16**, 387 (2019).